Article

Shape Change of Mineral Inclusions in Diamond—The Result of Diffusion Processes

Valentin Afanasiev [1,*], Sargylana Ugapeva [2] and Alla Logvinova [1]

1   Sobolev Institute of Geology and Mineralogy, Siberian Branch of the Russian Academy of Science, Koptyuga Pr. 3, Novosibirsk 630090, Russia; logv@igm.nsc.ru
2   Diamond and Precious Metal Geology Institute, Siberian Branch, Russian Academy of Science, Lenina Ave. 39, Yakutsk 677000, Russia; igabm@bk.ru
*   Correspondence: avp-diamond@mail.ru; Tel.: +7(913)-910-46-95

Abstract: The paper considers the possibility of changing the morphology of inclusions in diamonds based on the study of these inclusions and the inclusion–diamond boundary. Raman spectroscopy and transmission electron microscopy methods were used. According to the literature data, it is known that the octahedral form of mineral inclusions in diamond is induced, and does not correspond to the initial conditions of joint growth of diamond and inclusion, but the mechanism of this process is not considered. Solids differ in the value of surface Gibbs energy; the harder the material, the higher its melting point and the greater the value of surface Gibbs energy In the case of the diamond–inclusion pair, the surface energy of diamond far exceeds the surface energy of the inclusion. Diamond crystals have a surface energy value for an octahedron face of 5.3 J/m^2, dodecahedron—6.5 J/m^2, and cube—9.2 J/m^2, i.e. it is anomalously high compared to the surface tension of silicate and other minerals. Therefore, the mineral inclusion in diamond tends to the form corresponding to the minimum of free energy in the "diamond–inclusion" pair, and when the energy of diamond dominates, the final shape will be determined by it, i.e. it will be an octahedron. The authors suggest the possibility of redistribution of diamond substance around the inclusion with simultaneous change of the inclusion morphology.

Keywords: diamond; inclusion; morphology; diffusion; Raman spectroscopy; transmission electron microscopy (TEM)

1. Introduction

Inclusions in deep minerals from kimberlites serve as a source of important genetic information. They are considered as protogenetic, syngenetic and epigenetic. The former are rare and difficult to diagnose. The latter are widely presented and are considered as the main source of information about mineral paragenesis and the conditions of its formation. Still others are also widespread and are mainly represented by solid solution breakdown structures, reflecting evolution of the mineral in connection with the change of conditions of existence (late epigenetic inclusions related to the penetration of matter through cracks are not considered here). But in truth it is not always possible to reliably determine the genesis of inclusion. We have shown in the work [1] needle-like inclusions resulting from the breakdown of a solid solution of pyropes, that is, epigenetic inclusions can transform their shape and lose morphological signs of breakdown origin, and they can easily be mistaken for syngenetic ones. The picroilmenite lamellae of breakdown of a solid solution, represented by the spinel phase, as a result of morphological transformation, can form of chromite of octahedral shape and then there is a possibility of error–consideration of the paradoxical paragenesis "picroil-menite-chromite" [1]. The shape of inclusions in deep minerals is transformed due to diffusion mechanisms at high temperature and pressure [1]. At the same time, the signs of growth zoning are destroyed: deep minerals associated with the origin of mantle rocks have no growth zoning which is related to intramineral diffusion

processes [2]. In general, the associations of deep minerals from kimberlites show high lability in their structure and adaptability to the changing environmental conditions [1].

The only exception is the diamond. Every diamond crystal has a perfectly pronounced zoning that is clearly visible in cathodoluminescence or structural etching patterns. This indicates that its structure is very resistant to external influences. At the same time, the diamond does not have dead structure; it is also characterized by internal diffusion processes. They are expressed in the aggregation of a structural admixture of nitrogen and other impurities. Diamond annealing under high pressure and temperature conditions bring into action diffusion processes and the redistribution of impurity centers [3–5].

Diffusion processes cannot help but affect the substance of inclusions in diamonds. Inclusions are strictly isolated in the diamond matrix and all processes associated with them have an isochemical nature. Analogous to other deep minerals, it can be assumed that the driving force behind the transformation of inclusions in diamonds will be diffusion processes that lead to a change in the morphology of inclusions. But changing the shape of the inclusion requires a simultaneous change in the distribution of the diamond substance around the inclusion. B.A. Malkov and A.M. Askhabov [6] suggested that the octahedral faceting of inclusions of various minerals in diamonds [7,8] may be the result of a diffusion transformation of the initial shape of inclusions in accordance with the structure of the diamond, but they did not consider the mechanisms of transformation of the shape of inclusions and made a judgement only on the xenogenicity of diamonds. It is assumed that such a diffusion was facilitated by high temperatures in the diamond formation area and, probably, by the fluid phase inclusions in diamonds [9,10]. We found mineral inclusions in diamonds from the Aikhal kimberlite pipe and the Ebelyakh River placer [11,12], which indicate possible changes in their morphology within the diamond. The continuation of the search made it possible to find similar inclusions in many diamonds from different regions. Taking into account the structure and properties of diamond, we tried to understand the possibility of the processes of inclusion morphology change in diamond, relying mainly on the study of inclusion morphology and the inclusion–diamond boundary.

Nimis [13] investigated solid inclusions in lithospheric diamonds from Siberia and the Kaapvaal craton, using confocal micro-Raman spectroscopy and X-ray tomography. Fluid films including silicates $Si_2O(OH)_6$, $Si(OH)_4$ and water H_2O are present at the inclusion–diamond boundary. Fluid inclusions are abundant in cubic habit diamonds characterized by fibrous growth [14–17], but they are often found in other types of diamonds [9,18–23]. Water-containing medium has been proved to be effective for the formation of mantle diamonds and also contribute to diffusion processes inside diamonds [23]. These data, along with the study of the morphology of inclusions in diamonds, give reason to consider the possibility of changing the shape of inclusions from the point of view of minimizing the specific surface of inclusions and in general, minimizing the energy at the diamond–inclusion boundary as a thermodynamically conditioned process.

The importance of this work is that the evolution of inclusion morphology is used as an example to show the features of internal development of diamonds associated with diffusion processes. The morphology of inclusions is considered as a consequence of these processes and reflects the "maturity" of the diamond structure, i.e. the degree of change in the internal structure of diamond under the influence of external factors, primarily temperature and pressure of the external environment.

2. Materials and Methods

Diamonds with olivine inclusions were selected for the study, around which there were no cracks with exits to the face surface, or tiny, optically visible cracks appearing from the inclusions. At the same time, the inclusions had morphological features that could indicate the transformation of their morphology after the completion of diamond growth.

The morphological study of inclusions was carried out using optical microscopy, and its purpose is to trace the possible forms of transformation of the morphology of inclusions in diamonds.

Raman spectroscopy is used to identify inclusions in situ and study the composition of the fluid phase at the diamond–inclusion boundary. Nonpolarized Raman spectra were recorded in the range of 100–4000 cm^{-1} on a LabRam YR800 spectrometer with a 1024-channel LN/CCD detector in confocal mode using the microscope Olympus BX 4. A solid-state neodymium laser with a wavelength of 532 nm was used for the spectra excitation. The exposure time was 5 s, accumulating 5 scanned images. Measurements were carried out for the diamond itself, the inclusion of olivine in the diamond and the diamond–inclusion boundary. In addition, Raman mapping of the diamond–inclusion boundary was carried out. Mapping of the diamond–olivine boundary was carried out on the INTEGRA SPECTRUM measuring complex. A 100x lens with a numerical aperture of NA = 0.7 was used. Raman spectra were recorded by a CCD camera with cooling to −70 °C. For measurements, a mode with a signal accumulation time at each point of 50 s is selected, and the wavelength of the exciting radiation of a solid-state neodymium laser of 532 nm and a helium-neon gas laser of 632.8 nm, beam power with a diameter of <1 microns ~3.5 MW and ~3 MW, respectively. Raman mapping was carried out in 0.5 μm measurement intervals. Mapping was carried out by the area x−y (15 × 15 μm) at the depth of the inclusion z (~50–60 μm). The mapping area covered the diamond–inclusion contact area.

Images of the diamond–inclusion boundary were obtained using transmission electron microscopy on a Tecnai F20 X-Twin electron microscope at an accelerating voltage of 200 kW. In combination with the method of analytical electron spectroscopy (AES), the chemical composition of individual mineral phases at the "diamond–inclusion" boundary was determined. An energy dispersive spectrometer (EDAX) with an ultra-thin window of 3.8 nm, with a sample tilt angle of 20° and an exposure time of 200 seconds was used. For this purpose, using a special technique (FIB) described in [24,25], high-quality super-thin slices with dimensions of 15 × 8 × 0.15 microns were made.

3. Results

3.1. Morphological Research

Diamonds containing inclusions that indicate possible stages of transformation were chosen for the study. In the diamond from the placer of the Ebelyakh river (Arctic zone of the Siberian platform, crystal 6034), there is an inclusion of olivine with a pinch in the middle part (Figure 1a). This is a typical picture of the initial stage of decay of elongated inclusions into a number of fragments, followed by their transformation into isometric crystals, as described by Y.E. Geguzin [26]. We found similar inclusions with pinches in pyrope from kimberlite (Figure 1b) [1]. Small inclusions are visible around the inclusion in the diamond (Figure 1a), but at some distance from the large inclusion. This may be a consequence of coalescence of small inclusions into a large one, and because of this, the space around a large inclusion is cleared, and small inclusions remain only at a distance. A similar pattern was observed for picroilmenite with the breakdown of a solid solution from the Zimnaya pipe of the Upper Muna kimberlite field [1].

In the diamond 2004 from the Aikhal pipe, there are pinches on the elongated olivine inclusion, which are probably the initial stage of decay of the inclusion into fragments with their subsequent isometrization (Figure 2a).

In diamond 2114 from the Aikhal pipe, one can see the almost completed decayed process of an elongated inclusion with the isometrization of fragments (Figure 2b). We observed a similar pattern in pyrope [1]. An example of a chain of inclusions that developed along the twinning plane of a spinel twin is shown in Figure 2c (diamond 3156 from the Udachnaya pipe). The curved shape of the chain is probably related to its formation in the twinning plane with a high degree of defect.

Figure 3 shows photos of the inclusion of garnet and chromdiopside of an octahedral shape, which, according to our assumption, corresponds to the final stages of formation of the inclusion morphology. However, with special study, the signs of morphological transformation of inclusions can be found in many cases.
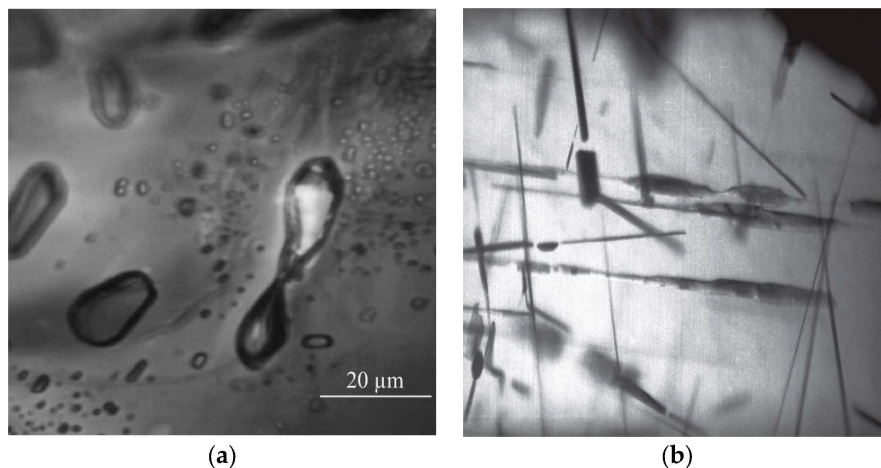
Figure 1. The initial stage of decay of elongated inclusions: (**a**)—silicate inclusion (olivine) with a pinch in diamond (crystal 6034); (**b**)—for comparison: similar pinches on the needle-like inclusion of an ore mineral in pyrope [1].
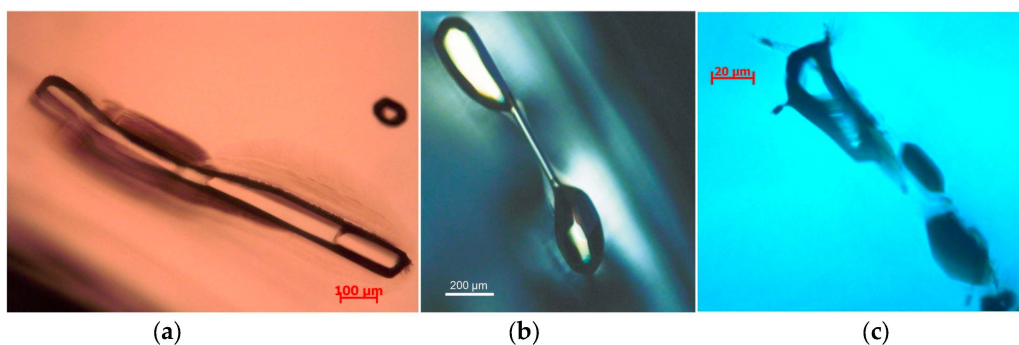

Figure 2. Olivine inclusions in diamonds: (**a**)—elongated inclusion of olivine with pinches (diamond 2004, the Aikhal pipe); (**b**)—fragments of the decayed inclusion (diamond 2114 from the Aikhal pipe); and (**c**)—fragmented inclusion of olivine in the twinning plane of a spinel twin (diamond 3156 from the Udachnaya pipe).
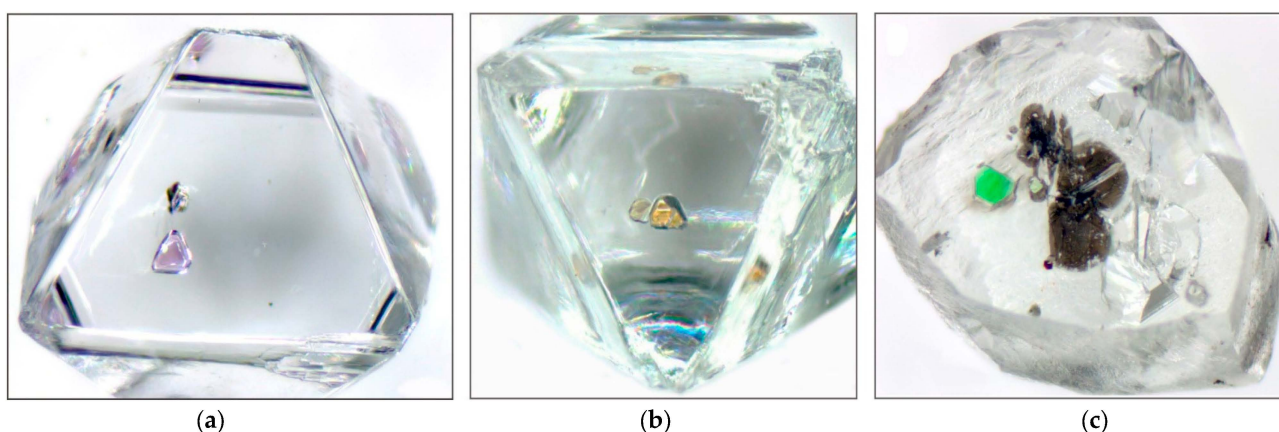

Figure 3. Octahedral shape of garnet inclusions in diamonds: (**a**) diamond of peridotite paragenesis with purple chromic garnet, (**b**) diamond of eclogite paragenesis with orange garnet, and (**c**) diamond with chromdiopside.

3.2. Raman Spectroscopy

Two diamond crystals from the Udachnaya pipe were studied by Raman spectroscopy: spinel twin of diamond 3156 with a chain of small colorless transparent inclusions and a

3230 diamond of octahedral habit with five transparent colorless inclusions located at different depths. Point spectra were obtained in the "diamond", "inclusion", "diamond–inclusion boundary" areas (Figure 4a,b). The Raman spectra of inclusions correspond to olivine with a characteristic doublet 824–825 and 855–857 cm^{-1} (Figure 4a, spectrum 3; Figure 4b, spectrum 2) [27]. In all of the obtained spectra, there is an intense Raman scattering signal of the first order from the diamond 1332cm^{-1} (sp^3-bonds), as well as a few less intensive bands (~1850, 2020, 2460 and 2670 cm^{-1}), related to second-order peaks (Figure 4) [28]. The spectra of the diamond–inclusion boundaries are characterized by two main broad peaks at 650–680 cm^{-1} and 760–830 cm^{-1} (Figure 4a, spectrum 2; Figure 4b, spectrum 4). The observed bands correspond to the monomers $Si(OH)_4$ (780–830 cm^{-1}) and dimers $Si_2O(OH)_6$ (650–680 cm^{-1}) in the aquatic environment according to [13,29,30]. These broad bands are accompanied by less intensive ones in the areas ~1675 cm^{-1} and 3595 cm^{-1} [31]. The band in the area of ~800 cm^{-1} corresponds to the symmetrical Si–O stretching in the monomer $Si(OH)_4$. The dimer frequencies in the area of ~600 cm^{-1} corresponding to symmetric stretching depend on the magnitude of the Si–O–Si angle and decrease with the increase of this angle. As shown in a number of papers, the peak frequencies corresponding to Si–O and Si–O–Si fluctuations depend on pressure and temperature [29] and on the chemical composition of a specific local solvation medium [13,30].
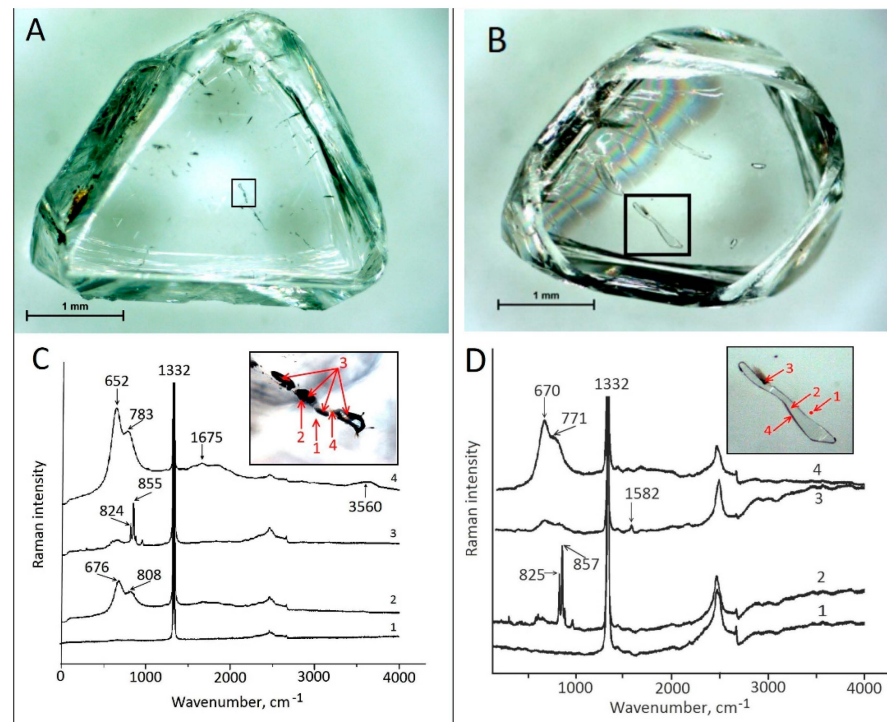

Figure 4. Raman spectra of diamond crystals 3156 (**A**) and 3230 (**B**). The inserts show photos of olivine inclusions in the areas indicated in (**A**) and (**B**). The numbering of the spectra corresponds to the points on the inserts. (**C**): 1—diamond, 2—diamond–olivine boundary (silicic fluid film), 3—olivine spectrum, and 4—the area of the halo between the olivines. (**D**): 1—diamond, 2—olivine (the olivine spectra are identical along the entire inclusion), 3—the area adjacent to the diamond–olivine boundary, and 4—diamond–olivine boundary (silicic fluid film).

A diamond crystal 5051 (The Sytykanskaya pipe) with a colorless transparent inclusion of olivine was studied by Raman mapping. Mapping was carried out on the area x-y (15 × 15 μm) at the depth of the inclusion stay z (~50–60 μm) (Figure 5a,b). The mapping area covered the diamond–inclusion contact area. The diamond–inclusion contact zone is clearly visible in the Raman mapping image (bright yellow) (Figure 5b). In the Raman spectrum of this area, wide bands of 658–788 cm^{-1} appear, corresponding, as noted above, to the $Si(OH)_4$ monomer and $Si_2O(OH)_6$ dimers in a water environment (Figure 5c) [13,29,30].

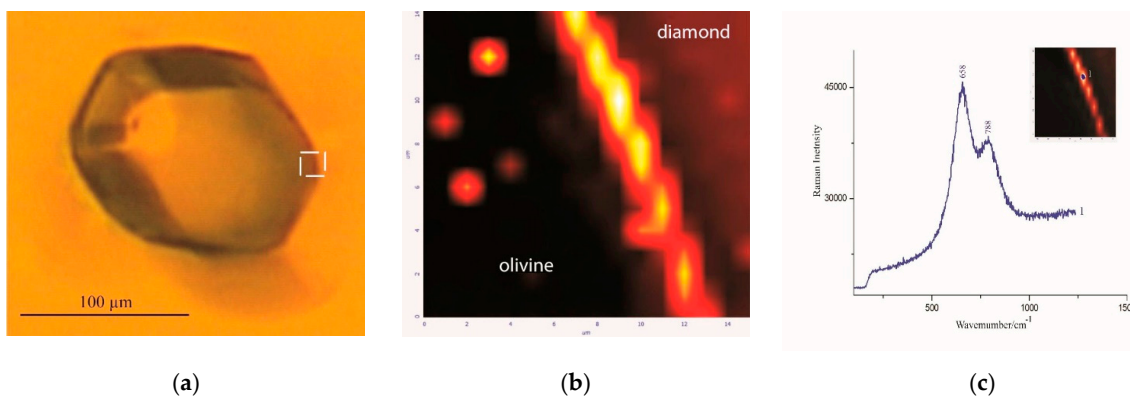At the same time, the thickness of the layer where the aforementioned bands appear varies from 1.5 to 4.5 μm.

(**a**)　　　　　　　　　　　(**b**)　　　　　　　　　　　(**c**)

Figure 5. Raman mapping of a diamond crystal 5051: (**a**) photo of olivine inclusion (the mapping area is highlighted with a white square); (**b**) image of the diamond–olivine boundary, Raman mapping; and (**c**) Raman spectrum of the diamond–inclusion contact zone (1).

3.3. Transmission Electron Microscopy (TEM)

To study the structure of the boundary between the mineral inclusion and diamond, thin sections of 10 × 15 μm were made on the boundary of olivine (Ud-56) and Cr-diopside (Ud-75) inclusions with a diamond matrix (Figure 6). The width of the boundary between the studied minerals and diamond is 20–50 nm. When the slice is made, the fluid evaporates and a solid material remains along the mineral–diamond boundary, which has an increased silica content (Figure 6c). Along the boundary on the olivine side, fluid bubbles, which have not yet been opened, were recorded (Figure 6b). The TEM results confirm the presence of the fluid phase at the mineral–diamond boundary.
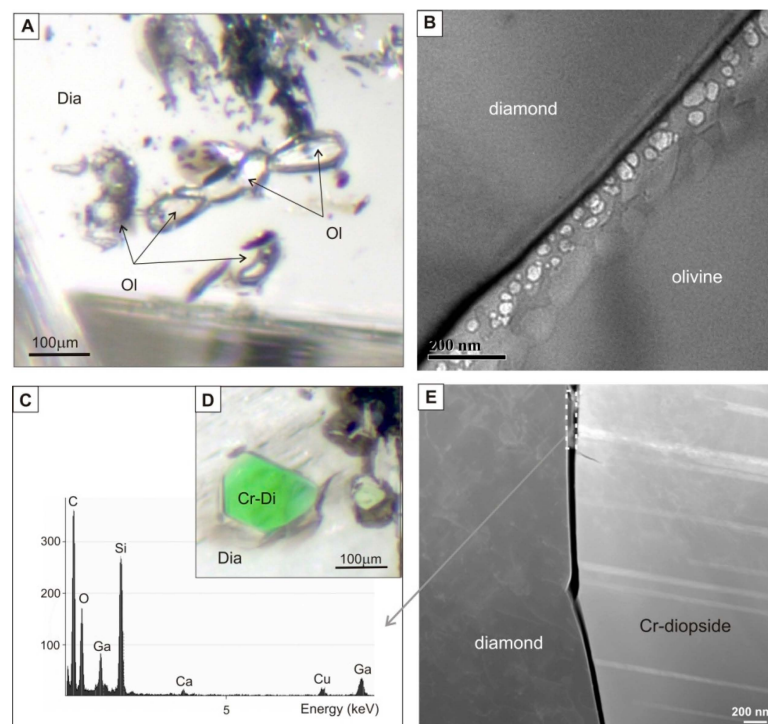

Figure 6. Micrography of olivine inclusions in diamond from the Udachnaya pipe (Ud-56) (**A**). TEM image of the boundary of olivine inclusion and diamond matrix; fluid inclusions are marked along the

boundary (**B**). Energy dispersion spectrum of the residual substance (**C**) at the boundary of inclusion of diopside and diamond matrix (**E**), and micrograph of Cr-diopside inclusion in diamond Ud-75 (**D**).

4. Discussion

This paper presents only a few examples that can be interpreted from the viewpoint of the diffusion transformation of the morphology of inclusions inside the diamond. But in reality, mineral inclusions in diamonds often show specific morphological signs indicating the possibility of transforming their morphology. In [8] it is indicated that the octahedral shape of garnet inclusions in diamond is induced, which does not correspond to the initial conditions of joint growth of diamond and garnet; however, the mechanism of this process is not considered. Octahedral inclusions in diamonds are also described in [7].

The transformation of the shape of inclusions in the deep minerals of kimberlites—pyropes, picroilmenites, chromites—is quite clear; it is described in detail and illustrated by us in [1]. In these cases, the host mineral and inclusion have comparable surface properties, and signs of diffusive mass transfer are widely manifested. Solids differ in the value of the Gibbs surface energy; the harder the material, the higher its melting point and the greater the value of surface Gibbs energy. In the case of the "diamond–inclusion" pair, the surface energy of the diamond is much higher than the surface energy of the inclusion. Diamond crystals have a surface energy value of 5.3 J/m^2 for the face of an octahedron, 6.5 J/m^2 for a dodecahedron and 9.2 J/m^2 for a cube [32] which is abnormally high compared to the surface tension of silicate and ore minerals; for example, for olivine faces (001) and (010), this value is 1.26 and 0.98, J/m^2, respectively [33]. Thermodynamic equilibrium assumes the achievement of a minimum of free energy (Gibbs energy), which includes the surface energy of the phases of the system. Therefore, the mineral inclusion in the diamond tends to the form corresponding to the minimum of free energy in the "diamond–inclusion" pair, and with the dominance of diamond energy, the final shape will be determined by it, i.e. this shape will be an octahedron. Therefore, the main question is the possibility of diffusive mass transfer of the diamond substance around the inclusion.

It was mentioned above that the preservation of the growth zoning is evidence of the conservatism of the diamond structure. The growth zoning is formed when the growth parameters change and is fixed by damages of the diamond structure, which are well expressed in the pattern of structural etching and cathodoluminescence [34]. Such defects are quite stable. But diffusion processes are widely manifested, which cause the redistribution and aggregation of structural nitrogen impurities, as well as other structural impurities [3–5] et al.

The plastic deformation of diamonds is also evidence of the possibility of diffusion processes. Deformed diamonds contain such mechanical defects as faults, irrational and regular twins, reorientation bands, and rotational dislocations [35]. Such defects are currently explained by dislocation mechanisms. The reverse process is also observed—the ordering of the diamond structure after plastic deformation in the form of polygonization and sometimes recrystallization [35]. Under high temperature conditions, dislocations are redistributed with the formation of dislocation sub-boundaries, i.e. a banded substructure of reflexes on lauegrams is formed [35].

Thus, diffusion processes occur in diamonds, so it can be assumed that the diamond substance, at least on the scale of the near order, has the ability to move.

Accordingly, it is possible to assume the possibility of redistribution of the diamond substance around the inclusion with a simultaneous change in the morphology of the inclusion. This is facilitated by the high permeability of the "diamond–inclusion" interphase boundary, as well as the presence of a fluid phase, which, due to its surface-active properties, serves as a conductor of the substance in the proposed processes of transformation of the shape of inclusions. The amorphization of olivine at the fluid boundary (plasticization) also indicates the activity of this boundary. The growth zoning of the diamond, as sufficiently stable, can be preserved at a distance from inclusions, whereas in the zones around inclusions, the latter can change morphology together with the diamond

matrix through diffusion processes. In cathodoluminescence patterns, whitish structureless halos are always observed around inclusions; perhaps they are related to the redistribution of the diamond substance around the inclusion. Since the surface energy of a diamond significantly exceeds the surface energy of any solid inclusion, the diamond "imposes" its morphology on inclusion in the process of diffusive transformation of its morphology.

Careful attention to the diamond shows that this mineral behaves like other minerals and obeys the general laws of mineral behavior. One can try to compare the behavior of inclusions in diamonds with the behavior of inclusions in kimberlite garnets described in [1]. In this work, the process of changing the shape of inclusions formed during the breakdown of a solid solution of garnet is characterized. Initially, flat accumulations of emulsion-like, amoeboid particles of an isotropic phase of indeterminate mineral affiliation are formed; accumulations are oriented along the rhombododecahedron. A possible analogue of such inclusions are small inclusions in the diamond in Figure 1a. Then begins the process of merging particles: formation of small, quite clearly individualized numerous inclusions of a new phase, which, in turn, in the process of coalescence form different needle-like inclusions. A similar inclusion in the diamond is shown in Figure 1b. Further evolution follows the path of breaking the needles into segments, tightening, isomerizing them, re-coalescence and the formation of large isometric inclusions, that is, the process seems to be repeated, but at a higher level. This orientation of the change in the shape of inclusions is due to a decrease in their specific surface area as they merge and, in general, a decrease in the elastic energy associated with them. Ultimately, as a result of long-term development, inclusions may lose the primary signs of origin as a result of the breakdown of a solid solution. We perceive them as independent and refer to syngenetic inclusions. All processes of transformation of inclusions in minerals are carried out in the solid phase and are theoretically described by Y.E. Geguzin (1975) [26].

Diamond is stoichiometrically an extremely pure mineral and solid solution decay structures are not observed in it. But elongated olivine inclusions, as in Figures 1, 2 and 6, are common and oriented subparallel to the octahedron edge [11,12]. Such inclusions are primarily subjected to fragmentation and further transformation of the morphology of fragments. Inclusions of other mineral phases with nonequilibrium morphology are primarily elongated and flattened, captured during growth, in accordance with our hypothesis, and are subject to epigenetic morphological transformations corresponding to those described above for pyropes from kimberlites.

The example with inclusions in pyrope shows only the possibilities and ways of transforming the morphology of inclusions in diamonds. Some similarities can be seen in a series of our illustrations: Figures 1–3. However, the specific forms of transformations may differ. They will depend on the size, initial shape, distribution of inclusions in diamond, as well as on the duration of the process of diffusive transformation of inclusion morphology. The activation energy of diffusion processes in diamond is much higher than in indicator minerals of kimberlites, so these processes may not end with the formation of octahedral inclusions.

It should be noted that the crystallographic orientation of inclusions both in indicator minerals of kimberlites [1] and diamonds [36] can be arbitrary.

Thus, according to our hypothesis, the octahedral shape of inclusions is the result of a long process of the morphology transformation of inclusions of different minerals within diamonds, regardless of the initial morphology and crystallographic orientation of these inclusions. Consequently, octahedral inclusions indicate the "maturity" of the diamond structure, its orderliness.

5. Conclusions

A hypothesis explaining the possibility of inclusions' shape transformation by diffusion inside diamond after its growth in deep conditions is proposed. The decisive significance in this process is the fluid phase at the diamond–inclusion boundary, which serves as a conductor of substance of both diamond and inclusion. The hypothesis is based

on natural observations and requires further specialized study of various inclusions from this point of view. Studies in this direction will allow us to better understand the genesis of inclusions, in particular, the octahedral shape of many, including polymineral, inclusions.

References

1. Afanasiev, V.P.; Zinchuk, N.N.; Pokhilenko, N.P. *Morphology and Morphogenesis of Kimberlite Indicator Minerals*; "Geo" Branch of SB RAS, "Manuscript" Publishing House: Novosibirsk, Russia, 2001; 276p.
2. Pokhilenko, N.P.; Afanasiev, V.P.; Agashev, A.M.; Pokhilenko, L.N.; Tychkov, N.S. Lithospheric mantle composition and structure variations under the Siberian platform kimberlite fields of different ages. *Geodyn. Tectonophys.* **2022**, *13*, 666. [CrossRef]
3. Bokiy, G.B.; Bezrukov, G.N.; Klyuev, Y.A.; Naletov, A.M.; Nepsha, V.I. *Natural and Synthetic Diamonds*; Nauka: Moscow, Russia, 1986; 270p.
4. Chepurov, A.I.; Fedorov, I.I.; Sonin, V.M. *Experimental Modeling of Diamond Formation Processes*; SPCJIGGM SB RAS Publishing House: Novosibirsk, Russia, 1997; 160p.
5. Zaitsev, A.M. *Optical Properties of Diamond: A Data Handbook*; Springer-Verlag: Berlin/Heidelberg, Germany, 2001; 502p.
6. Malkov, B.A.; Askhabov, A.M. Crystal inclusions with octahedral faceting (negative crystals)—Evidence of xenogenic origin of diamonds in kimberlites. *Dokl. Earth Sci. USSR* **1978**, *238*, 695–699.
7. Sobolev, N.V.; Botkunov, A.I.; Bakumenko, I.T.; Sobolev, V.S. Crystal inclusions with octahedral faceting in diamonds. *Dokl. Earth Sci. USSR* **1972**, *204*, 192–195.
8. Bartoshinsky, Z.V.; Efimova, E.S.; Zhikhareva, V.P.; Sobolev, N.V. Crystallomorphology of garnet inclusions in natural diamonds. *Geol. Geophys.* **1980**, *3*, 12–22.
9. Giardini, A.A.; Melton, C.E. Experimental results and theoretical interpretation of gaseous inclusions found in Arkansas natural diamonds. *Am. Mineral.* **1975**, *60*, 413–417.
10. Melton, C.E.; Giardini, A.A. Experimental evidence that oxygen in principal impurity in natural diamonds. *Nature* **1976**, *263*, 309–310. [CrossRef]
11. Ugapieva, S.S.; Pavlushin, A.D.; Goryainov, S.V. Typomorphic characteristics of diamond crystals with olivine inclusions from the Ebelyakh placer and kimberlite bodies of the Yakutian diamond-bearing province. *Nauka I Obraz.* **2015**, *2*, 28–34.
12. Ugapieva, S.S.; Pavlushin, A.D.; Goryainov, S.V.; Afanasiev, V.P.; Pokhilenko, N.P. Comparative characteristics of diamonds with olivine inclusions from the Ebelyakh placer and kimberlite bodies of the Yakutian diamond-bearing province. *Dokl. Earth Sci.* **2016**, *468*, 473–477. [CrossRef]
13. Nimis, P.; Alvaro, M.; Nestola, F.; Angel, R.J.; Marquardt, K.; Rustioni, G.; Harris, J.W.; Marone, F. First evidence of hydrous silicic fluid films around solid inclusions in gem-quality diamonds. *Lithos* **2016**, *260*, 384–389. [CrossRef]
14. Navon, O.; Hutcheson, I.D.; Rossman, G.R.; Wasserburg, G.J. Mantle-derived fluids in diamond micro-inclusions. *Nature* **1988**, *335*, 784–789. [CrossRef]
15. Logviniva, A.M.; Wirth, R.; Fedorova, E.N.; Sobolev, N.V. Nanometer-sized mineral and fluid inclusions in cloudy Siberian diamonds: New insights on diamond formation. *Eur. J. Mineral.* **2008**, *20*, 317–331. [CrossRef]
16. Klein-Ben David, O.; Graham Pearson, D.; Nowell, G.M.; Ottley, C.; McNeill, J.C.R.; Logvinova, A.; Sobolev, N.V. The sources and time-integrated evolution of diamondforming fluids—Trace elements and Sr isotopic evidence. *Geochim. Cosmochim. Acta* **2014**, *125*, 146–169. [CrossRef]
17. Logvinova, A.M.; Zedgenizov, D.A.; Wirth, R. Specific Multiphase Assemblages of Carbonatitic and Al-Rich Silicic Diamond-Forming Fluids/Melts: TEM Observation of Microinclusions in Cuboid Diamonds from the Placers of Northeastern Siberian Craton. *Minerals* **2019**, *9*, 50. [CrossRef]
18. Tomlinson, E.L.; Jones, A.P.; Harris, J.W. Co-existing fluid and silicate inclusions in mantle diamond. *Earth Planet. Sci. Lett.* **2006**, *250*, 581–595. [CrossRef]
19. Logvinova, A.M.; Wirth, R.; Tomilenko, A.A.; Afanas'ev, V.P.; Sobolev, N.V. The phase composition of crystal-fluid nanoinclusions in alluvial diamonds in the northeastern Siberian Platform. *Geol. Geophys.* **2011**, *52*, 1286–1297. [CrossRef]

20. Evan, M. Smith, Maya G. Kopylova, Geoff M. Nowell, D. Graham Pearson, and John Ryder. Archean mantle fluids preserved in fibrous diamonds from Wawa, Superior craton. *Geology* **2012**, *40*, 1071–1074. [CrossRef]

21. Smith, E.M.; Kopylova, M.G.; Frezzotti, M.L.; Afanasiev, V.P. Fluid inclusions in Ebelyakh diamonds: Evidence of CO_2 liberation in eclogite and the effect of H_2O on diamond habit. *Lithos* **2015**, *216–217*, 106–117. [CrossRef]

22. Sobolev, N.V.; Logvinova, A.M.; Tomilenko, A.A.; Wirth, R.; Bul'bak, T.A.; Luk'yanova, L.I.; Fedorova, E.N.; Reutsky, V.N.; Efimova, E.S. Mineral and fluid inclusions in diamonds from the Urals placers, Russia: Evidence for solid molecular N2 and hydrocarbons in fluid inclusions. *Geochim. Cosmochim. Acta* **2019**, *266*, 197–219. [CrossRef]

23. Stachel, T.; Luth, R.W. Diamond formation—Where, when and how? *Lithos* **2015**, *220–223*, 200–220. [CrossRef]

24. Wirth, R. Focused Ion Beam (FIB): A novel technology for advanced application of micro- and nanoanalysis in geosciences and applied mineralogy. *Eur. J. Mineral.* **2004**, *16*, 863–876. [CrossRef]

25. Wirth, R. Focused Ion Beam (FIB) combined with SEM and TEM: Advanced analytical tools for studies of chemical composition, microstructure and crystal structure in geomaterials on a nanometre scale. *Chem. Geol.* **2009**, *261*, 217–229. [CrossRef]

26. Geguzin, Y.E. Mechanisms and kinetics of transformation of the shape of inclusions in crystals. In *Problems of Modern Crystallography. Collection of Articles in Memory of Academician A.V. Shubnikov*; Nauka: Moscow, Russia, 1975; pp. 110–127.

27. Yasuzuka, T.; Ishibashi, H.; Arakawa, M.; Yamamoto, J.; Kagi, H. Simultaneous determination of Mg# and residual pressure in olivine using micro-Raman spectroscopy. *J. Mineral. Petrol. Sci.* **2009**, *104*, 395–400. [CrossRef]

28. Windl, W.; Pavone, P.; Karch, K. Second-order Raman spectra of diamond from ab-initio phonon calculation. *Phys. Rev. B* **1993**, *48*, 31–64. [CrossRef] [PubMed]

29. Zotov, N.; Keppler, H. Silica speciation in aqueous fluids at high pressures and high temperatures. *Chem. Geol.* **2002**, *184*, 71–82. [CrossRef]

30. Hunt, J.D.; Kavner, A.; Schauble, E.A.; Snyder, D.; Manning, C.E. Polymerization of aqueous silica in $H_2O–K_2O$ solutions at 25–200 °C and 1 bar to 20 kbar. *Chem. Geol.* **2011**, *283*, 161–170. [CrossRef]

31. Ratcliffe, C.; Irish, D. Vibrational spectral studies of solutions at elevated temperatures and pressures. 5. Raman studies of liquid water up to 300 °C. *J. Phys. Chem.* **1982**, *86*, 4897–4905. [CrossRef]

32. Field, J.E. *Properties of Diamond*; Academic Press: New York, NY, USA; London, UK, 1979; 674p.

33. Swain, M.V.; Atkinson, B.K. Fracture surface energy of olivine. *Pure Appl. Geophys.* **1978**, *116*, 866–872. [CrossRef]

34. Afanasiev, V.; Ugapeva, S.; Babich, Y.; Sonin, V.; Logvinova, A.; Yelisseyev, A.; Goryainov, S.; Agashev, F.; Ivanova, O. History of Diamond growth: A Window to the Lithospheric Mantle. *Minerals* **2022**, *12*, 1048. [CrossRef]

35. Rylov, G.M.; Fedorova, E.N.; Sobolev, N.V. Investigation of the internal structure of imperfect diamond crystals based on the Laue–SE synchrotron method. *Geol. Geophys.* **2006**, *47*, 242–249.

36. Sobolev, N.V.; Seryotkin Yu, V.; Logvinova, A.M.; Pavlushin, A.D.; Ugap'eva, S.S. Crystallographic orientation and geochemical specifics of mineral inclusions in diamonds. *Russ. Geol. Geophys.* **2020**, *61*, 774–793. [CrossRef]